Stable isotopic evidence for the excess leaching of unprocessed atmospheric nitrate from forested catchments under high nitrogen saturation

Weitian Ding[1], Urumu Tsunogai[1], Fumiko Nakagawa[1], Takashi Sambuichi[1], Masaaki Chiwa[2], Tamao Kasahara[3], Ken'ichi Shinozuka[4]

[1]Graduate School of Environmental Studies, Nagoya University, Furo-cho, Chikusa-ku, Nagoya 464-8601, Japan

[2]Kyushu University Forest, Kyushu University, Japan

[3]Faculty of Agriculture, Kyushu University, Japan

[4]River Basin Research Center, Gifu University, 1-1 Yanagido, Gifu, 501-1193, Japan

Corresponding author: Weitian Ding

Email: ding.weitian.v2@s.mail.nagoya-u.ac.jp

Abstract

Owing to the elevated loading of nitrogen through atmospheric deposition, some forested ecosystems become nitrogen saturated, from which elevated levels of nitrate are exported. The average concentration of stream nitrate eluted from upstream and downstream of the Kasuya Research forested catchments (FK1 and FK2 catchments) in Japan were more than 90 μM, implying that these forested catchments were under nitrogen saturation. To verify that these forested catchments were under the nitrogen saturation, we determined the export flux of unprocessed atmospheric nitrate relative to the entire deposition flux (M_{atm}/D_{atm} ratio) in these catchments, because the M_{atm}/D_{atm} ratio has recently been proposed as a reliable index to evaluate nitrogen saturation in forested catchments. Specifically, we determined the temporal variation in the concentrations and stable isotopic compositions, including $\Delta^{17}O$, of stream nitrate in the FK catchments for more than 2 years. In addition, for comparison, the same parameters were also monitored in the Shiiba Research forested catchment (MY catchment) in Japan during the same period, where the average stream nitrate concentration was low, less than 10 μM. While showing the average nitrate concentrations of 109.5, 90.9, and 7.3 μM in FK1, FK2, and MY, respectively, the catchments showed average $\Delta^{17}O$ values of +2.6, +1.5, and +0.6 ‰ in FK1, FK2, and MY, respectively. Thus, the average concentration of unprocessed atmospheric nitrate ($[NO_3^-{}_{atm}]$) was estimated to be 10.8, 5.1, and 0.2 μM in FK1, FK2, and MY, respectively, and the M_{atm}/D_{atm} ratio was estimated to be 14.1, 6.6, and 1.3 % in FK1,

FK2, and MY, respectively. The estimated M_{atm}/D_{atm} ratio in FK1 (14.1 %) was the highest ever reported from temperate forested catchments monitored for more than 1 year. Thus, we concluded that nitrogen saturation was responsible for the enrichment of stream nitrate in the FK catchments, together with the elevated $NO_3^-{}_{atm}$ leaching from the catchments. While the stream nitrate concentration ($[NO_3^-]$) can be affected by the amount of precipitation, the M_{atm}/D_{atm} ratio is independent of the amount of precipitation; thus, the M_{atm}/D_{atm} ratio can be used as a robust index for evaluating nitrogen saturation in forested catchments.

1 Introduction

Nitrate is important as a nitrogenous nutrient in the biosphere. Traditionally, forested ecosystems have been considered as nitrogen limited (Vitousek and Howarth, 1991). However, owing to the elevated loading of nitrogen through atmospheric deposition, some forested ecosystems become nitrogen saturated (Aber et al., 1989), from which elevated levels of nitrate are exported (Mitchell et al., 1997; Peterjohn et al., 1996). Such excessive leaching of nitrate from forested catchments degrades water quality and causes eutrophication in downstream areas (Galloway et al., 2003; Paerl and Huisman, 2009). Thus, evaluating the stage of nitrogen saturation in each forested catchment including its temporal variation, is critical for sustainable forest management, especially for forested ecosystems under high nitrogen deposition.

Both concentration and seasonal variation of stream nitrate have been used as indexes

to evaluate the nitrogen saturation of each forested catchment in past studies (Aber, 1992; Rose et al., 2015; Stoddard, 1994). A forested stream eluted from Fernow Experimental Forest USA, for instance, showed an elevated average nitrate concentration of 60 μM, along with the absence of a seasonal variation in the stream nitrate concentration, so the forest was classified into stage 3, the highest stage of nitrogen saturation (Rose et al., 2015).

However, using both the concentration level (high or low) and seasonal variation (clear or absent) of stream nitrate as indexes to evaluate nitrogen saturation has limitations, including the following (1) seasonal variation of soil nitrate can be buffered by groundwater with long residence time, so that the seasonal variation is unclear in stream nitrate concentration in Japan, even in normal forests under the nitrogen saturation stage of 0 (Mitchell et al., 1997); and (2) the stream nitrate concentration can be enriched or diluted depending on the volume of rainfall, so the concentration level can be high in low precipitation area irrespective of the stage of nitrogen saturation.

Nakagawa et al. (2018) lately proposed that the M_{atm}/D_{atm} ratio, the export flux of unprocessed atmospheric nitrate (M_{atm}) relative to the deposition flux of $NO_3^-{}_{atm}$ (D_{atm}), can be an alternative, more robust index for evaluating nitrogen saturation in each forested catchment, because the M_{atm}/D_{atm} ratio directly reflects the demand for atmospheric nitrate deposited onto each forested catchments as a whole, and thus reflect the nitrogen saturation in each forested catchment. That is, we can expect high M_{atm}/D_{atm} ratios in forested catchments under nitrogen saturation and low M_{atm}/D_{atm}

ratios in forested catchments with nitrogen deficiency.

To estimate the M_{atm}/D_{atm} ratio accurately and precisely in each forested catchment, the fraction of unprocessed atmospheric nitrate ($NO_3^-{}_{atm}$) in the stream needs to be estimated accurately and precisely. Triple oxygen isotopic compositions of nitrate ($\Delta^{17}O$) have recently been used as a conservative tracer of $NO_3^-{}_{atm}$ deposited onto each forested catchment (Inoue et al., 2021; Michalski et al., 2004; Nakagawa et al., 2018; Tsunogai et al., 2014; Ding et al., 2022), showing distinctively different $\Delta^{17}O$ from that of remineralized nitrate ($NO_3^-{}_{re}$), derived from organic nitrogen through general chemical reactions, including microbial N mineralization and microbial nitrification. While $NO_3^-{}_{re}$, the oxygen atoms of which are derived from either terrestrial O_2 or H_2O through microbial processing (i.e., nitrification), always shows the relation close to the "mass-dependent" relative relation between $^{17}O/^{16}O$ ratios and $^{18}O/^{16}O$ ratios; $NO_3^-{}_{atm}$ displays an anomalous enrichment in ^{17}O reflecting oxygen atom transfers from atmospheric ozone (O_3) during the conversion of NO_X to $NO_3^-{}_{atm}$ (Alexander et al., 2009; Michalski et al., 2003; Morin et al., 2011; Nelson et al., 2018). As a result, the $\Delta^{17}O$ signature defined by the following equation (Kaiser et al., 2007) enables us to distinguish $NO_3^-{}_{atm}$ ($\Delta^{17}O > 0$) from $NO_3^-{}_{re}$ ($\Delta^{17}O = 0$):

$$\Delta^{17}O = \frac{1+\delta^{17}O}{(1+\delta^{18}O)^{\beta}} - 1 \quad (1)$$

where the constant β is 0.5279 (Kaiser et al., 2007), $\delta^{18}O = R_{sample}/R_{standard} - 1$ and R is the $^{18}O/^{16}O$ ratio (or the $^{17}O/^{16}O$ ratio in the case of $\delta^{17}O$ or the $^{15}N/^{14}N$ ratio in the case of $\delta^{15}N$) of the sample and each standard reference material. In addition, $\Delta^{17}O$ is almost

87 stable during “mass-dependent” isotope fractionation processes within terrestrial
88 ecosystems. Therefore, while the $\delta^{15}N$ or $\delta^{18}O$ signature of $NO_3^-{}_{atm}$ can be overprinted
89 by the biological processes subsequent to deposition, $\Delta^{17}O$ can be used as a robust tracer
90 of unprocessed $NO_3^-{}_{atm}$ to reflect its accurate mole fraction within total NO_3^-,
91 regardless of the progress of the partial metabolism (partial removal of nitrate through
92 denitrification and assimilation) subsequent to deposition (Michalski et al., 2004;
93 Nakagawa et al., 2013, 2018; Tsunogai et al., 2011, 2014, 2018).
94 Past studies reported that the maximum concentration of stream nitrate was 58.4 μM
95 in the KJ forested catchment in Japan, with the maximum value of the M_{atm}/D_{atm} ratio
96 was 9.4 % (Nakagawa et al., 2018; Sase et al., 2022). Whether the index of the M_{atm}/D_{atm}
97 ratio can be applied to forested catchments, where the leaching of stream nitrate is much
98 higher than the KJ forested catchment, remained unclarified. Besides, the advantages
99 of the M_{atm}/D_{atm} ratio within the past indexes of nitrogen saturation have not been
100 discussed.
101 Chiwa (2021) has recently reported the enrichment of nitrate of more than 90 μM on
102 the annual average in forested streams eluted from the FK catchments (FK1 and FK2)
103 in Kasuya Research Forest, Kyushu University, Japan (Figs. 1a and 1b). The observed
104 enrichment of stream nitrate implied that these forested catchments were under nitrogen
105 saturation. Thus, in this study, we determined the M_{atm}/D_{atm} ratio in the FK1 and FK2
106 forested catchments by monitoring both the concentration and $\Delta^{17}O$ of stream nitrate
107 for more than 2 years to verify that these forested catchments were under nitrogen

saturation. For comparison, the MY forested catchment in Shiiba Research Forest, Kyushu University, Japan (Figs. 1a and 1c), was also monitored during the same period, where the average stream nitrate concentration was low (less than 10 μM). Furthermore, the M_{atm}/D_{atm} ratios in these forested catchments were compared with those reported in past studies to verify the reliability of the M_{atm}/D_{atm} ratio as an index of nitrogen saturation.

2 Methods

2.1 Study sites

The FK forested catchments (33°38′N, 130°31′E) are located in a suburban area, about 15 km west of the Fukuoka metropolitan area (the fourth largest metropolitan area in Japan). The main plantation in these catchments was Japanese cedar/cypress (Table 1). The MY forested catchment (32°22′N, 131°09′E) is located in a rural area at the village of Shiiba in southern Japan's Central Kyushu Mountain range. This catchment is a mixed forest consisting of coniferous trees such as *Abies firma Sieb. et Zucc.,* and *Tsuga sieboldii Carr.,* and deciduous broadleaved trees such as *Quercus crispula Blume*, *Fagus crenata Blume*, and *Acer sieboldianum* Miq. Details on the studied forested catchments have been described in the past studies (Chiwa, 2020, 2021).

2.2 Sampling

The stream water eluted from the FK1 (14 ha), FK2 (62 ha), and MY (43 ha)

129 forested catchments were collected about once every month in principle from 2019/11
130 to 2021/12 (Fig. 1). At the FK catchments, stream water was collected at upstream
131 (station A) and downstream (station B) locations (Fig. 1b). At the MY catchment,
132 stream water was collected at station C (Fig. 1c). Samples of stream water to determine
133 the concentration and stable isotopic compositions ($\delta^{15}N$, $\delta^{18}O$, and $\Delta^{17}O$) of stream
134 nitrate were collected manually in bottles washed with deionized water before sampling
135 and then rinsed at least twice with the sample before sampling at each sampling site.
136
137 2.3 Analysis
138 All the stream water samples were passed through a membrane filter (pore size 0.45
139 μm) within two days after sampling and stored in a refrigerator (4 °C) until analysis.
140 The concentrations of nitrate were measured by ion chromatography (Prominence HIC-
141 SP, Shimadzu, Japan). To determine the stable isotopic compositions of nitrate in the
142 stream water samples, nitrate in each sample was chemically converted to N_2O using a
143 method originally developed to determine the $^{15}N/^{14}N$ and $^{18}O/^{16}O$ ratios of seawater
144 and freshwater nitrate (McIlvin and Altabet, 2005) that was later modified (Konno et
145 al., 2010; Tsunogai et al., 2011; Yamazaki et al., 2011). In brief, 11 mL of each sample
146 solution was pipetted into a vial with a septum cap. Then, 0.5 g of spongy cadmium
147 was added, followed by 150 μL of a 1 M $NaHCO_3$ solution. The sample was then shaken
148 for 18-24 h at a rate of 2 cycles s^{-1}. Then, the sample solution (10 mL) was decanted
149 into a different vial with a septum cap. After purging the solution using high-purity

150 helium, 0.4 mL of an azide–acetic acid buffer, which had also been purged using high-
151 purity helium, was added. After 45 min, the solution was alkalinized by adding 0.2 mL
152 of 6 M NaOH. Then, the stable isotopic compositions ($\delta^{15}N$, $\delta^{18}O$, and $\Delta^{17}O$) of the
153 N_2O in each vial were determined using the continuous-flow isotope ratio mass
154 spectrometry (CF-IRMS) system at Nagoya University. The analytical procedures
155 performed using the CF-IRMS system were the same as those detailed in previous
156 studies (Hirota et al., 2010; Komatsu et al., 2008a). The obtained values of $\delta^{15}N$, $\delta^{18}O$,
157 and $\Delta^{17}O$ for the N_2O derived from the nitrate in each sample were compared with those
158 derived from our local laboratory nitrate standards to calibrate the values of the sample
159 nitrate to an international scale and to correct for both isotope fractionation during the
160 chemical conversion to N_2O and the progress of oxygen isotope exchange between the
161 nitrate derived reaction intermediate and water (ca. 20 %). In this study, we adopted the
162 internal standard method to calibrate the stable isotopic compositions of sample nitrate.
163 Specifically, three kinds of the local laboratory nitrate standards were used in this study,
164 which were named to be GG01 ($\delta^{15}N$ = –3.07 ‰, $\delta^{18}O$ = +1.10 ‰, and $\Delta^{17}O$ = 0 ‰),
165 HDLW02 ($\delta^{15}N$ = +8.94 ‰, $\delta^{18}O$ = +24.07 ‰), and NF ($\Delta^{17}O$ = +19.16 ‰), which the
166 GG01 and the HDLW02 were used to determine the $\delta^{15}N$ and $\delta^{18}O$ of stream nitrate,
167 and the GG01 and the NF was used to determine the $\Delta^{17}O$ of stream nitrate. The GG01,
168 HDLW02, and NF had been calibrated using the internationally distributed isotope
169 reference materials (USGS 34 and USGS 35). The oxygen exchange rate between
170 nitrate and water during the chemical conversion was calculated through Eq. (2):

171 Oxygen exchange rate (%) = $\Delta^{17}O(N_2O)_{NF}$ / $\Delta^{17}O(NO_3^-)_{NF}$ (2)

172 where the $\Delta^{17}O(N_2O)_{NF}$ denote the $\Delta^{17}O$ value of N_2O that convert from the NF

173 nitrate, the $\Delta^{17}O(NO_3^-)_{NF}$ denote the $\Delta^{17}O$ value of NF nitrate ($\Delta^{17}O$ = +19.16 ‰)

174 (Tsunogai et al., 2016; Nakagawa et al., 2013, 2018; Ding et al., 2022).

175 The δ^2H and $\delta^{18}O$ values of H_2O of the stream water samples were analyzed using

176 the cavity ring-down spectroscopy method by employing an L2120-i instrument

177 (Picarro Inc., Santa Clara, CA, USA) equipped with an A0211 vaporizer and

178 autosampler. The errors (standard errors of the mean) in this method were ±0.5‰ for

179 δ^2H and ±0.1‰ for $\delta^{18}O$. Both the VSMOW and standard light Antarctic precipitation

180 (SLAP) were used to calibrate the values to the international scale. The $\delta^{18}O$ values of

181 H_2O were used to calibrate the differences in $\delta^{18}O$ of H_2O between the samples and

182 those our local laboratory nitrate standard samples (Tsunogai et al., 2010, 2011, 2014).

183 To determine whether the conversion rate from nitrate to N_2O was sufficient, the

184 concentration of nitrate in the samples was determined each time we analyzed the

185 isotopic composition using CF-IRMS based on the N_2O^+ or O_2^+ outputs. We adopted

186 the $\delta^{15}N$, $\delta^{18}O$, and $\Delta^{17}O$ values only when the concentration measured via CF-IRMS

187 correlated with the concentration measured via ion chromatography prior to isotope

188 analysis within a difference of 10 %. We repeated the analysis of $\delta^{15}N$, $\delta^{18}O$, and $\Delta^{17}O$

189 values for each sample at least three times to attain high precision. All samples had a

190 nitrate concentration of greater than 3.5 μM, which corresponded to a nitrate quantity

191 greater than 35 nmol in a 10 mL sample. Thus, all isotope values presented in this study

have an error (standard error of the mean) better than ±0.2 ‰ for $\delta^{15}N$, ±0.3 ‰ for $\delta^{18}O$, and ±0.1 ‰ for $\Delta^{17}O$.

Nitrite (NO_2^-) in the samples interferes with the final N_2O produced from nitrate because the chemical method also converts NO_2^- to N_2O (McIlvin and Altabet, 2005). Therefore, it is sometimes necessary to remove NO_2^- prior to converting nitrate to N_2O. In this study, however, we skipped the processes for removing NO_2^- because all the stream samples analyzed for stable isotopic composition had NO_2^- concentrations lower than the detection limit (0.05 μM).

2.4 Deposition rate of atmospheric nitrate

The annual deposition rate of atmospheric nitrate (D_{atm}; total dry and wet deposition rate of atmospheric nitrate) in each catchment was estimated using the annual "bulk" deposition rate of atmospheric nitrate (D_{bulk}) calculated in Chiwa (2020) at each catchment by multiplying the volume-weighted mean concentration of nitrate in the bulk deposition samples collected every 2 weeks at each catchment for 10 years (from 2009/1 to 2018/12) by the annual amount of precipitation. The bulk deposition samples were those accumulated in a plastic bucket installed in an open site of each catchment 55 cm above the ground. The distances between the monitoring sites of bulk deposition in the FK1, FK2, and MY forested catchments and the stations of stream water sampling (stations A, B, and C) were 3.9, 2.9, and 4.5 km, respectively. The concentrations of nitrate in the bulk deposition samples were measured by ion chromatography.

The D_{bulk} determined through this method, however, is less than D_{atm} (Aikawa et al., 2003) because the dry deposition velocities of gases and particles on the water surface of the plastic bucket are smaller than those on the forest (Matsuda, 2008). Thus, we corrected the differences by using Eq. (3) to estimate D_{atm} from D_{bulk}:

$$D_{atm} = D_{bulk} - D_{dry}(W) + D_{dry}(F) \quad (3)$$

where $D_{dry}(W)$ and $D_{dry}(F)$ denote the annual dry deposition rates onto water and forest, respectively.

The $D_{dry}(W)$ and $D_{dry}(F)$ at each catchment were determined using an inferential method (Endo et al., 2011) through Eqs. (4) and (5), respectively:

$$D_{dry}(W) = [NO_3^-{}_{atm}]_{gas} \times V_{gas}(W) + [NO_3^-{}_{atm}]_p \times V_p(W) \quad (4)$$

$$D_{dry}(F) = [NO_3^-{}_{atm}]_{gas} \times V_{gas}(F) + [NO_3^-{}_{atm}]_p \times V_p(F) \quad (5)$$

where $[NO_3^-{}_{atm}]_{gas}$ denotes the concentration of gaseous nitrate in air; $[NO_3^-{}_{atm}]_p$ denotes the concentration of particle nitrate in air; $V_{gas}(W)$ and $V_{gas}(F)$ denote the deposition velocities of gaseous nitrate on the water surface and forest, respectively; and V_p (W) and V_p (F) denote the deposition velocities of particulate nitrate on the water surface and forest, respectively. Those determined by Chiwa (2010) using the annular denuder method from 2006/5 to 2007/4 were used for the $[NO_3^-]_{gas}$ and $[NO_3^-]_p$ in the FK catchments. Those determined by the National Institute for Environmental Studies (Environmental Laboratories Association of Japan, 2017) using the filter-pack method at Miyazaki (31°83′N, 131°42′E) from 2011 to 2017 were used for the $[NO_3^-]_{gas}$ and $[NO_3^-]_p$ in the MY catchment. The $V_{gas}(F)$, $V_{gas}(W)$, $V_p(F)$, and $V_p(W)$ of each

234 catchment were determined by applying the estimation file for dry deposition (Matsuda,
235 2008;
236 http://www.hro.or.jp/list/environmental/research/ies/katsudo/acid_rain/kanseichinchak
237 u/kanseichinchaku.html), where V_{gas} and V_p were calculated using the meteorological
238 data of wind speed, temperature, humidity, radiation, and cloud amount and land use.
239 The meteorological data monitored by Japan Meteorological Agency at the nearest
240 Fukuoka station (33°34′N, 130°22′E) and Miyazaki station (31°56′N, 131°24′E) from
241 2009 to 2021 were used for the FK and MY catchments, respectively. The forested land
242 use of 100 % was chosen for each area.
243
244 2.5 Flux of stream water
245 The flux of stream water (F_{stream}) in each catchment was not measured fully in this
246 study. Instead, the water balance in each catchment was used to estimate F_{stream},
247 assuming that the outflux of water from the study catchments to deep groundwater was
248 negligible:
249 $F_{stream} = P - E$ (6)
250 where P denotes the annual average precipitation and E denotes the annual
251 evapotranspiration flux of water in each catchment. In this paper, the equation obtained
252 by Komatsu et al. (2008) was used to estimate the E of the FK and MY catchments.
253 Details on this equation are shown below.
254 Komatsu et al. (2008) compiled the annual flux of evapotranspiration determined in

43 forested catchments in Japan and found that E shows a positive correlation with the average temperature (T_{avg}) of each catchment. Thus, they proposed the modeled relation of E (mm) = 31.4T_{avg} (°C) + 376 to estimate E in each forested catchment in Japan, where the standard error of 162.3 mm was included in the estimated evapotranspiration flux (E). They also confirmed that the estimated F_{stream} using the model corresponded well with the observed F_{stream} in three forested catchments, with estimated errors of less than 6 %. As a result, we utilized the water balance method proposed by Komatsu et al. (2008) to quantify the F_{stream} in each catchment.

2.6 Concentration of unprocessed $NO_3^-{}_{atm}$ in each water sample

The $\Delta^{17}O$ data of nitrate in each sample was used to estimate the concentration of $NO_3^-{}_{atm}$ ($[NO_3^-{}_{atm}]$) in each water sample by applying Eq. (7):

$$[NO_3^-{}_{atm}]/[NO_3^-] = \Delta^{17}O/\Delta^{17}O_{atm} \quad (7)$$

where $[NO_3^-{}_{atm}]$ and $[NO_3^-]$ denote the concentrations of $NO_3^-{}_{atm}$ and nitrate (total) in each water sample, respectively, and $\Delta^{17}O_{atm}$ and $\Delta^{17}O$ denote the $\Delta^{17}O$ values of $NO_3^-{}_{atm}$ and nitrate (total) in the stream water sample, respectively. In this study, we used the annual average $\Delta^{17}O$ value of $NO_3^-{}_{atm}$ determined at the Sado-Seki monitoring station in Japan (Sado Island; Fig. 1a) from April 2009 to March 2012 ($\Delta^{17}O_{atm}$ = +26.3 ‰; Tsunogai et al., 2016) for $\Delta^{17}O_{atm}$ in Eq. (7) to estimate $[NO_3^-{}_{atm}]$ in the stream. We allow for an error range of 3 ‰ in $\Delta^{17}O_{atm}$, where the factor changes in $\Delta^{17}O_{atm}$ from +26.3 ‰ caused by both areal and seasonal variations in the $\Delta^{17}O$ values of

276 $NO_3^-{}_{atm}$ have been considered (Nakagawa et al., 2018; Tsunogai et al., 2016; Ding et
277 al., 2022).
278 The annual export flux of unprocessed $NO_3^-{}_{atm}$ per unit area of the catchment (M_{atm})
279 was determined by applying Eq. (8):
280 $$M_{atm} = [NO_3^-{}_{atm}]_{avg} \times F_{stream} \quad (8)$$
281 where $[NO_3^-{}_{atm}]_{avg}$ denotes the annual average $[NO_3^-{}_{atm}]$ in each stream. The index of
282 nitrogen saturation (M_{atm}/D_{atm} ratio) was calculated by dividing M_{atm} with D_{atm} in each
283 catchment.
284
285 2.7 Concentration and isotopic compositions of stream nitrate eluted only from the FK2
286 catchment
287 The concentration and isotopic compositions ($\delta^{15}N$, $\delta^{18}O$, and $\Delta^{17}O$) of stream nitrate
288 determined at station B were the mixtures of those eluted from FK1 and FK2
289 catchments (Fig. 1b). Assuming that the stream nitrate eluted from FK1 catchment was
290 stable during the flow path from station A to station B. The concentration of stream
291 nitrate eluted from the FK2 catchment was determined by applying Eq. (9):
292 $$[NO_3^-]_{FK2} = ([NO_3^-]_{FK1+FK2} * F_{FK1+FK2} - [NO_3^-]_{FK1} * F_{FK1}) / F_{FK2} \quad (9)$$
293 where F_{FK1}, F_{FK2}, and $F_{FK1+FK2}$ denote the flux of stream water eluted from the FK1,
294 FK2 (only), and FK1+FK2 catchment, respectively. $[NO_3^-]_{FK1}$, $[NO_3^-]_{FK2}$, and
295 $[NO_3^-]_{FK1+FK2}$ denote the concentration of stream nitrate eluted from the FK1, FK2
296 (only), and FK1+FK2 catchment, respectively. In this study, the flow rates measured at

297 stations A and B on 2021/01/15 by using the salt dilution method (Sappa et al., 2015)
298 was used for F_{FK1} (0.85 L/s) and $F_{FK1+FK2}$ (4.75 L/s), respectively, and the measured
299 $[NO_3^-]$ at stations A and B was used for $[NO_3^-]_{FK1}$ and $[NO_3^-]_{FK1+FK2}$, respectively.
300 Because the relation between the measured flow rates was comparable with the relation
301 between the catchment area of FK1 (14 ha) and that of FK1+FK2 (76 ha), we concluded
302 that the measured flow rates of 0.85 L/s and 4.75 L/s were reasonable as for those
303 representing the F_{FK1} and $F_{FK1+FK2}$, respectively. According to the mass balance of water,
304 we can estimate the F_{FK2} eluted from the FK2 catchment only to be 3.90 L/s.
305 Assuming that the stream nitrate eluted from FK1 catchment was stable during the
306 flow path from station A to station B, the $\delta^{15}N$, $\delta^{18}O$, and $\Delta^{17}O$ values of stream nitrate
307 eluted from the FK2 catchment only were determined by applying Eq. (10):
308 $\delta_{FK2} = (\delta_{FK1+FK2} * [NO_3^-]_{FK1+FK2} * F_{FK1+FK2} - \delta_{FK1} * [NO_3^-]_{FK1} * F_{FK1}) / ([NO_3^-]_{FK2} *$
309 $F_{FK2})$ (10)
310 where δ_{FK1}, δ_{FK2}, and $\delta_{FK1+FK2}$ denote the $\delta^{15}N$ (or $\delta^{18}O$ or $\Delta^{17}O$) of stream nitrate eluted
311 from the FK1, FK2, and FK1+FK2 catchment, respectively. The $\delta^{15}N$ (or $\delta^{18}O$ or $\Delta^{17}O$)
312 values of stream nitrate measured at stations A and B were used for δ_{FK1} and $\delta_{FK1+FK2}$,
313 respectively.
314
315 **3 Results**
316 3.1 Deposition rate of atmospheric nitrate
317 The mean annual precipitation (P) from 2009 to 2021 was 1777 mm and 3981 mm

for FK and MY catchments, respectively (Chiwa, 2020; Chiwa, personal communication, September 21, 2022). The mean annual temperature (T_{avg}) was reported to be 15.9 °C and 10.8 °C for FK and MY catchments, respectively (Chiwa, 2020). Based on these data, the annual flux of stream water (F_{stream}) was estimated to be 902.0 ± 162.3 mm at FK catchments and 3266.1 ± 162.3 mm at MY catchment, respectively, using Eq. (6).

Chiwa (2020) reported the annual bulk deposition rates of atmospheric nitrate (D_{bulk}) to be 34.0 mmol m^{-2} $year^{-1}$ at FK catchments and 24.2 mmol m^{-2} $year^{-1}$ at MY catchment. On the other hand, the annual dry deposition rate of atmospheric nitrate (D_{dry}) deposited on the forest ($D_{dry}(F)$) and on the water surface ($D_{dry}(W)$) were estimated to be 39.9 mmol m^{-2} $year^{-1}$ and 4.1 mmol m^{-2} $year^{-1}$, respectively, at FK catchments, and 18.4 mmol m^{-2} $year^{-1}$ and 2.4 mmol m^{-2} $year^{-1}$, respectively, at MY catchment. As a result, D_{atm} was estimated to be 69.3 mmol m^{-2} $year^{-1}$ at FK catchments and 40.1 mmol m^{-2} $year^{-1}$ at MY catchment, using Eq. (3).

3.2 Concentration and isotopic composition of stream nitrate

The concentrations of stream nitrate eluted from the FK1, FK2 (only), and MY catchments ranged from 97.5 μM to 121.3 μM, from 65.7 μM to 148.5 μM, and from 3.5 μM to 15.3 μM, respectively, with the average concentrations of 109.5 μM, 90.9 μM, and 7.3 μM, respectively, and the standard deviations (SD) of 6.3 μM, 18.5 μM, and 3.0 μM, respectively, which corresponds to the coefficients of variation (CV) of

339 5.7 %, 20.4 %, and 40.7 %, respectively (Fig. 2a). All catchments showed no clear
340 seasonal variation during the observation periods. The variation ranges and the average
341 concentrations of stream nitrate eluted from the three catchments agreed well with the
342 past observations performed in the same catchments (Chiwa, 2021).

343 The stable isotopic compositions of stream nitrate eluted from the FK1, FK2 (only),
344 and MY catchments ranged from −0.9 ‰ to +1.5 ‰, from −1.4 ‰ to +5.8 ‰, and from
345 −0.8 ‰ to +2.4 ‰, respectively, for $\delta^{15}N$ (Fig. 2b), from +3.9 ‰ to +8.5 ‰, from −2.2 ‰
346 to +2.8 ‰, and from −5.6 ‰ to +1.7 ‰, respectively, for $\delta^{18}O$ (Fig. 2c), and from +2.0 ‰
347 to +3.3 ‰, from +0.6 ‰ to +2.2 ‰, and from +0.2 ‰ to +1.0 ‰, respectively, for $\Delta^{17}O$
348 (Fig. 2d), with no clear seasonal variation during the observation periods. The
349 concentration-weighted averages for the $\delta^{15}N$, $\delta^{18}O$, and $\Delta^{17}O$ values of stream nitrate
350 were +0.2 ‰, +6.4 ‰, and +2.6 ‰, respectively, at FK1, +1.0 ‰, +0.5 ‰, and +1.5 ‰,
351 respectively, at FK2, +0.7 ‰, −2.5 ‰, and +0.6 ‰, respectively, at MY.

352

353 3.3 Concentration of unprocessed atmospheric nitrate and the M_{atm}/D_{atm} ratio in each
354 catchment

355 The concentration of unprocessed atmospheric nitrate ($[NO_3^-{}_{atm}]$) in the streams eluted
356 from the FK1, FK2 (only), and MY catchments ranged from 8.64 to 14.30 μM, from
357 2.27 to 10.71 μM, and from 0.03 to 0.46 μM with the average concentration of 10.80 ±
358 1.30, 5.06 ± 0.67, and 0.16 ± 0.03 μM, respectively, even though these studied
359 catchments showed little seasonal variations during the observation periods (Fig. 2e).

The annual export flux of nitrate (M_{total}), the annual export flux of $NO_3^-{}_{atm}$ (M_{atm}), and the M_{atm}/D_{atm} ratio were 98.8 ± 17.8 mmol m^{-2} $year^{-1}$, 9.7 ± 2.1 mmol m^{-2} $year^{-1}$, and 14.1 ± 4.1 % at FK1 catchment, respectively, 82.0 ± 14.8 mmol m^{-2} $year^{-1}$, 4.6 ± 1.0 mmol m^{-2} $year^{-1}$, and 6.6 ± 2.0 % at FK2 catchment, respectively, 23.7 ± 1.2 mmol m^{-2} $year^{-1}$, 0.5 ± 0.1 mmol m^{-2} $year^{-1}$, and 1.3 ± 0.4 % at MY catchment, respectively (Table 2). The uncertainties of [$NO_3^-{}_{atm}$], M_{atm}, and M_{atm}/D_{atm} ratio in each catchment were determined from the uncertainties of $\Delta^{17}O$, $\Delta^{17}O_{atm}$, F_{stream}, and D_{atm} according to the equations of error propagation. The details were described in Appendix A.

4 Discussion

4.1 Deposition rate of atmospheric nitrate at the study catchments

Based on the air monitoring data determined at the stations of Fukuoka (33°51′N, 130°50′E) and Miyazaki (31°83′N, 131°42′E) from 2011 to 2017, the Environmental Laboratories Association of Japan (2017) reported D_{atm} to be 57.8 mmol m^{-2} $year^{-1}$ at Fukuoka and 49.1 mmol m^{-2} $year^{-1}$ at Miyazaki. Those values are consistent with the D_{atm} estimated in this study (69.3 and 40.1 mmol m^{-2} $year^{-1}$ at the FK and MY catchments, respectively), within a difference of approximately 20 %. Thus, we concluded that the D_{atm} estimated in this study was reliable within the error margin of 20 % (Table 2). Because the D_{atm} determined at the FK catchments was the highest among the forested catchments in Table 3, we further compared the D_{atm} of the FK catchments with those from the other air monitoring stations in Japan reported in past

studies, along with that of the MY catchment (Table S1). While the D_{atm} of the MY catchment corresponded to the average level among the sites compiled in Table S1, the D_{atm} of the FK catchments exceeded the average level significantly. In addition, the D_{atm} of the FK catchments corresponded to one of the highest among the Japanese forested areas (Table S1). All the catchments in Japan can be suffered from the long-range transport of air pollutants derived from megacities in East Asian region (Chiwa, 2021; Chiwa et al., 2012 and 2013).In addition, the shorter transport distance from the Fukuoka metropolitan area (total population: 1.62 million people; population density: 4715 people/km^2) may be mainly responsible for the D_{atm} higher in FK than in MY, because the FK catchments are only 15 km west of the Fukuoka metropolitan area.

4.2 Excess leaching of unprocessed atmospheric nitrate from FK catchments

The isotopic compositions ($\delta^{15}N$, $\delta^{18}O$, and $\Delta^{17}O$) of stream nitrate eluted from the FK and MY catchments were typical for those eluted from forested catchments (Hattori et al., 2019; Huang et al., 2020; Nakagawa et al., 2013, 2018; Riha et al., 2014; Sabo et al., 2016; Tsunogai et al., 2014, 2016). The striking features found in the FK catchments were that, in addition to the high [NO_3^-] and high M_{total} that had been clarified in a past study (Chiwa, 2021), both [$NO_3^-{}_{atm}$] and M_{atm} in FK were higher than those eluted from MY (Table 2). Especially, the average [$NO_3^-{}_{atm}$] in the stream eluted from the FK1 catchment was the highest ever reported in forested streams determined through continuous monitoring for more than 1 year (Bostic et al., 2021; Bourgeois et al., 2018b,

2018a; Hattori et al., 2019; Huang et al., 2020; Nakagawa et al., 2018; Rose et al., 2015; Sabo et al., 2016; Tsunogai et al., 2014, 2016).

The observed high [$NO_3^-{}_{atm}$] in the stream eluted from the FK1 catchment could be caused just by the high [$NO_3^-{}_{atm}$] deposition in the catchment. Thus, we compiled all past data ever reported in forested streams through continuous monitoring in Table 3, where the data of average [NO_3^-], average [$NO_3^-{}_{atm}$], M_{atm}, M_{total}, D_{atm}, and M_{atm}/D_{atm} ratio were included for comparison. The result showed that the M_{atm}/D_{atm} ratio, along with M_{atm}, was the highest as well in the FK1 catchment among the forested catchments (Table 3).

Elevated loading of nitrogen through atmospheric deposition was responsible for the occurrence of nitrogen saturation in forest ecosystems, from which elevated levels of nitrate are exported (Aber et al., 1989). Nakagawa et al. (2018) proposed that the M_{atm}/D_{atm} ratio can be an index for evaluating the nitrogen saturation in each forested catchment, because the M_{atm}/D_{atm} ratio directly reflects the present demand for atmospheric nitrate deposited in each forested catchment, and thus reflects the nitrogen saturation in each forested catchment. The high M_{atm}/D_{atm} ratios observed in the FK catchments implied that the demand for atmospheric nitrate was low in the FK catchments and that the stages of nitrogen saturation at the FK catchments were higher than those at other forested catchments. That is, the nitrogen saturation at the FK catchments was responsible for the observed high [NO_3^-] and high M_{total} at the FK catchments than at MY and any other catchment ever studied (Table 3).

423 The stand age of forests can affect the retention or loss of N (Fukushima et al., 2011;
424 Ohrui and Mitchell, 1997). Fukushima et al. (2011) evaluated N uptake rates of
425 Japanese cedars at different ages (5-89 years old) and demonstrated that the N uptake
426 rates of Japanese cedars were higher in younger stands (53 kg N ha^{-1} $year^{-1}$ in 16 years
427 old) than in older stands (29 kg N ha^{-1} $year^{-1}$ in 31 years old; 24 kg N ha^{-1} $year^{-1}$ in 42
428 years old; 34 kg N ha^{-1} $year^{-1}$ in 89 years old). In addition, Yang and Chiwa (2021)
429 found that the nitrate concentration in the soil water taken beneath the rooting zone of
430 matured artificial Japanese cedar plantations (607 ± 59 μM; 64-69 years old) was
431 significantly higher than that of normal Japanese oak plantations (8.7 ± 8.1 μM; 24
432 years old). Moreover, by adding ammonium nitrate (50 kg N ha^{-1} $year^{-1}$) to the forest
433 floor directly, Yang and Chiwa (2021) found that the nitrate concentration in the soil
434 water of the matured artificial Japanese cedar plantations increased significantly faster
435 than that of the normal Japanese oak plantations, probably because of the lower N
436 uptake rates in the matured artificial Japanese cedar plantations. Because most of the
437 artificial Japanese cedar/cypress plantations in the FK and MY catchments have reached
438 their maturity (> 50 years; Yang and Chiwa, 2021), the higher proportion of matured
439 artificial Japanese cedar/cypress plantations in the FK1 catchment (Table 1) was highly
440 responsible for the observed elevated leaching of nitrate, caused by the reduction in N
441 uptake rates.

442 As a result, we concluded that the FK forested catchments were under the high
443 nitrogen saturation stage, FK1 catchment especially, and the nitrogen saturation in the

444 FK1 catchment was responsible for the elevated M_{total}, M_{atm}, [NO_3^-], [$NO_3^-{}_{atm}$] found
445 in the stream eluted from the catchment (Figs. 3a, 3b, 3c and 3d).
446
447 4.3 The M_{atm}/D_{atm} ratio as an index of nitrogen saturation
448 Past studies have used the concentration of stream nitrate as one of the important
449 indexes to evaluate the stage of nitrogen saturation in each forest (Aber, 1992; Huang
450 et al., 2020; Rose et al., 2015; Stoddard, 1994). The strong linear relationship ($R^2 = 0.76$;
451 $P < 0.0001$) between the stream nitrate concentration and the M_{atm}/D_{atm} ratio, except
452 for the Qingyuan forested catchment (Fig. 3d), further supported that the M_{atm}/D_{atm} ratio
453 can be used as an alternative index of nitrogen saturation, as pointed out in Nakagawa
454 et al. (2018).
455 The differences in the number of storm and/or snowmelt events could affect the
456 M_{atm}/D_{atm} ratio as well, because $NO_3^-{}_{atm}$ could be injected into the stream water directly,
457 along with the storm/snowmelt water (Tsunogai et al., 2014; Ding et al., 2022; Inamdar
458 and Mitchell, 2006). In recent study, however, we found that storm events have little
459 impact on the M_{atm}/D_{atm} ratio, based on monitoring temporal variation of [$NO_3^-{}_{atm}$] in
460 stream water during storm events (Ding et al., 2022). In addition, the low M_{atm}/D_{atm}
461 ratio found in Uryu forested catchment (0.7 %; Table 3) implied that the snowmelt has
462 little impact on the M_{atm}/D_{atm} ratio as well, because 30% of the annual mean
463 precipitation was snow in Uryu forested catchment (Tsunogai et al., 2014).
464 The differences in the amount of precipitation, temperature, and the flux of stream
465 water could affect the M_{atm}/D_{atm} ratio as well. As a result, the annual amount of

precipitation, mean temperature, and the annual mean flux of stream water (F_{stream}) in the forested catchments were compiled in Table S2. While the stream nitrate concentration showed a strong linear relationship (R^2 = 0.76; P < 0.0001) with the M_{atm}/D_{atm} ratio (Fig. 3d), the precipitation, temperature, and F_{stream} did not show a significant relationship with the M_{atm}/D_{atm} ratio (P > 0.14; Fig. 4). As a result, we concluded that the M_{atm}/D_{atm} ratio was mainly controlled by the progress of nitrogen saturation, rather than the differences in the number of storm and/or snowmelt events, the amount of precipitation, temperature, and the flux of stream water.

The differences in the residence time of water in each catchment could also impact the M_{atm}/D_{atm} ratio, as the residence time of water in forested catchments ranges from one month to more than one year (Asano et al., 2002; Farrick and Branfireun, 2015; Kabeya et al., 2008; Rodgers et al., 2005; Soulsby et al., 2006; Tetzlaff et al., 2007). It is difficult to explain high [NO_3^-] and high M_{total} eluted from the catchment by the residence time of water alone, while the M_{atm}/D_{atm} ratio could be higher in catchments with a shorter water residence time, as the majority of nitrate eluted from the catchment with a high M_{atm}/D_{atm} ratio was $NO_3^-{}_{re}$ produced by microbial nitrification. The significant correlation between M_{total} and M_{atm}/D_{atm} ratios (P < 0.0001; Fig. 3a) supported nitrogen saturation as the leading cause of high M_{total} in catchments with a high M_{atm}/D_{atm} ratio. Additionally, the high loading of atmospheric nitrogen, the type of plantation, and the old age of plantation in the FK1 catchment all supported the conclusion that the FK1 catchment was under nitrogen saturation.

The M_{atm}/D_{atm} ratio is a more reliable and robust index than the stream nitrate

concentration, as explained below. The Qingyuan forested catchment can be classified into the highest nitrogen saturation stage based only on the highest stream nitrate concentration of 150 μM (Table 3). However, based on the leaching flux of nitrogen via stream water monitored by Huang et al. (2020) for 4 years in the Qingyuan forested catchment, along with the deposition flux of nitrogen, we can obtain the M_{atm}/D_{atm} ratio in the catchment to be a medium level of 5.8 ± 1.3 %, implying that the nitrogen saturation stage was not so high (Table 3). Huang et al. (2020) also concluded that the input of nitrogen exceeded the output in the catchment, and thus, the catchment was at stage 2 of nitrogen saturation. The M_{atm}/D_{atm} ratio in the Qingyuan forested catchment with a medium level among all forested catchments (Fig. 3d) should be a more reliable index of nitrogen saturation.

Compared with those in the other forested catchments in Table 3, the annual amount of precipitation (P) has the lowest value of 709 mm in the Qingyuan forested catchment. The flux of stream water (F_{stream}) has the lowest value of 309 mm as well. Thus, we concluded that nitrate was relatively concentrated in the catchment because of the small precipitation, resulting in relative enrichment in the concentrations of both nitrate (150 μM) and unprocessed atmospheric nitrate (8.9 μM) in the stream.

While the concentration of stream nitrate, as an index of nitrogen saturation traditionally, can be influenced by the amount of precipitation, as demonstrated in the Qingyuan forested catchment, the M_{atm}/D_{atm} ratio is independent of the amount of precipitation (Fig. 4). Therefore, the M_{atm}/D_{atm} ratio can be used as a more robust index

for evaluating nitrogen saturation in each forested catchment.

5 Conclusions

Both the concentrations and $\Delta^{17}O$ of stream nitrate were determined for more than 2 years in the forested catchments of FK (FK1 and FK2) and MY to determine the M_{atm}/D_{atm} ratio for each catchment. The FK catchments exhibited higher M_{atm}/D_{atm} ratio than the MY catchment and other forested catchments reported in past studies, implying that the progress of nitrogen saturation in the FK catchments was severe. Both age and proportion of artificial plantation in the FK catchments were responsible for the progress of nitrogen saturation. In addition, although past studies have commonly used the concentration of stream nitrate as an index to evaluate the progress of nitrogen saturation in forested catchments, it can be influenced by the amount of precipitation. As a result, we concluded that the M_{atm}/D_{atm} ratio should be used as a more reliable index for evaluating the progress of nitrogen saturation because the M_{atm}/D_{atm} ratio is independent from the amount of precipitation.

Appendix A: Calculating of uncertainties in the values of $[NO_3^-{}_{atm}]$, M_{atm}, and M_{atm}/D_{atm} ratio

The uncertainty in the values of $[NO_3^-{}_{atm}]$ was estimated from the uncertainties in the $\Delta^{17}O$ values of stream nitrate ($\Delta^{17}O$) and $NO_3^-{}_{atm}$ ($\Delta^{17}O_{atm}$) according to the divisive equation of error propagation (A1):

$$\sigma_{[NO_3^-{}_{atm}]}=[NO_3^-]*\sqrt{\left(\frac{1}{\Delta^{17}O_{atm}}*\sigma_{\Delta^{17}O}\right)^2+\left(\frac{\Delta^{17}O}{\Delta^{17}O_{atm}{}^2}*\sigma_{\Delta^{17}O_{atm}}\right)^2} \quad (A1)$$

where $\sigma_{[NO_3^-{}_{atm}]}$, $\sigma_{\Delta^{17}O}$, and $\sigma_{\Delta^{17}O_{atm}}$ denote the uncertainties in $[NO_3^-{}_{atm}]$, $\Delta^{17}O$ values of stream nitrate, and $\Delta^{17}O$ values of $NO_3^-{}_{atm}$, respectively. The standard error of the mean (SE) of ±0.1 ‰ and the areal/seasonal variations of ±3 ‰ was used in calculating $\sigma_{\Delta^{17}O}$ and $\sigma_{\Delta^{17}O_{atm}}$, respectively. As a result, the uncertainty in $[NO_3^-{}_{atm}]$ ($\sigma_{[NO_3^-{}_{atm}]}$) was ±1.30, ±0.67, and ±0.03 μM at FK1, FK2, and MY catchments, respectively.

The uncertainty in the values of M_{atm} was estimated from the uncertainties in $[NO_3^-{}_{atm}]$ and in F_{stream} according to the multiplicative equation of error propagation (A2):

$$\sigma_{M_{atm}}=\sqrt{(F_{stream}*\sigma_{[NO_3^-{}_{atm}]})^2+([NO_3^-{}_{atm}]*\sigma_{F_{stream}})^2} \quad (A2)$$

where $\sigma_{M_{atm}}$, $\sigma_{[NO_3^-{}_{atm}]}$, and $\sigma_{F_{stream}}$ denote the uncertainties in M_{atm}, $[NO_3^-{}_{atm}]$, and F_{stream}, respectively. Komatsu et al. (2008) proposed the uncertainty in F_{stream} to be ±162.3 mm when using the water balance method in estimating F_{stream}. Here, the uncertainty in M_{atm} ($\sigma_{M_{atm}}$) was ±2.1, ±1.0, and ±0.1 mmol m^{-2} yr^{-1} at FK1, FK2, and MY catchments, respectively.

The uncertainty in M_{atm}/D_{atm} ratio was estimated from the uncertainties in M_{atm} and in D_{atm} according to the divisive equation of error propagation (A3):

$$\sigma_{M_{atm}/D_{atm}\ ratio}=\sqrt{\left(\frac{1}{D_{atm}}*\sigma_{M_{atm}}\right)^2+\left(\frac{M_{atm}}{D_{atm}{}^2}*\sigma_{D_{atm}}\right)^2} \quad (A3)$$

where $\sigma_{M_{atm}/D_{atm}\ ratio}$, $\sigma_{M_{atm}}$, and $\sigma_{D_{atm}}$ denote the uncertainty in M_{atm}/D_{atm} ratio, M_{atm}, and D_{atm}, respectively. Comparing the deposition rate of $NO_3^-{}_{atm}$ obtained at the other atmospheric monitoring stations nearby, the uncertainty of 20 % was adopted for those of D_{atm} in each catchment, which corresponds to the uncertainty in D_{atm} of ±13.9, ±13.9, ±8.0 mmol m^{-2} yr^{-1} at FK1, FK2, and MY catchments, respectively. As

554 a result, the uncertainty in M_{atm}/D_{atm} ratio was ±4.1 %, ±2.0 %, and ±0.4 % at FK1,
555 FK2, and MY catchments, respectively.

556

557 *Data availability.* All the primary data are presented in the Supplement. The other data
558 are available upon request to the corresponding author (Weitian Ding).

559

560 *Author contributions.* UT, FN, KS, and MC designed the study. MC and TK performed
561 the field observations. WD, UT, and FN determined the concentrations and isotopic
562 compositions of the samples. WD, TS, FN, and UT performed data analysis, and WD
563 and UT wrote the paper with input from MC, TK, and KS.

564

565 *Competing interests.* The authors declare that they have no conflict of interest.

566

567 *Acknowledgements.*
568 We thank anonymous referees for valuable remarks on an earlier version of this paper.
569 We also thank Daisuke Nanki, Takuma Nakamura, and Yuko Muramatsu for their
570 long-term water sampling. Additionally, we are grateful to the members of the
571 Biogeochemistry Group, Graduate School of Environmental Studies, Nagoya
572 University, for their valuable support throughout this study. This work was supported
573 by a Grant-in-Aid for Scientific Research from the Ministry of Education, Culture,
574 Sports, Science, and Technology of Japan under grant numbers 22H00561, and
575 17H00780, the Yanmar Environmental Sustainability Support Association, and the

River fund of the river foundation, Japan. Weitian Ding would like to take this opportunity to thank the “Nagoya University Interdisciplinary Frontier Fellowship” supported by Nagoya University and JST, the establishment of university fellowships towards the creation of science technology innovation, Grant Number JPMJFS2120.

Reference

Aber, J. D.: Nitrogen cycling and nitrogen saturation in temperate forest ecosystems, Trends Ecol. Evol., 7(7), 220–224, doi:10.1016/0169-5347(92)90048-G, 1992.

Aber, J. D., Nadelhoffer, K. J., Steudler, P. and Melillo, J. M.: Nitrogen Saturation in Northern Forest Ecosystems, Bioscience, 39(6), 378–386, doi:10.2307/1311067, 1989.

Aikawa, M., Hiraki, T., Tamaki, M. and Shoga, M.: Difference between filtering-type bulk and wet-only data sets based on site classification, Atmos. Environ., 37(19), 2597–2603, doi:10.1016/S1352-2310(03)00214-0, 2003.

Alexander, B., Hastings, M. G., Allman, D. J., Dachs, J., Thornton, J. A. and Kunasek, S. A.: Quantifying atmospheric nitrate formation pathways based on a global model of the oxygen isotopic composition ($\delta^{17}O$) of atmospheric nitrate, Atmos. Chem. Phys., 9(14), 5043–5056, doi:10.5194/acp-9-5043-2009, 2009.

Asano, Y., Uchida, T. and Ohte, N.: Residence times and flow paths of water in steep unchannelled catchments, Tanakami, Japan, J. Hydrol., 261(1–4), 173–192, doi:10.1016/S0022-1694(02)00005-7, 2002.

Environmental Laboratories Association of Japan: Acid Rain National Survey Report 2017, https://tenbou.nies.go.jp/envgis_explain/acid_rain/content.html.

Bostic, J. T., Nelson, D. M., Sabo, R. D. and Eshleman, K. N.: Terrestrial Nitrogen Inputs Affect the Export of Unprocessed Atmospheric Nitrate to Surface Waters: Insights from Triple Oxygen Isotopes of Nitrate, Ecosystems, doi:10.1007/s10021-021-00722-9, 2021.

Bourgeois, I., Savarino, J., Némery, J., Caillon, N., Albertin, S., Delbart, F., Voisin, D. and Clément, J. C.: Atmospheric nitrate export in streams along a montane to urban gradient, Sci. Total Environ., 633, 329–340, doi:10.1016/j.scitotenv.2018.03.141, 2018a.

Bourgeois, I., Savarino, J., Caillon, N., Angot, H., Barbero, A., Delbart, F., Voisin, D. and Clément, J. C.: Tracing the Fate of Atmospheric Nitrate in a Subalpine Watershed Using $\Delta^{17}O$, Environ. Sci. Technol., 52(10), 5561–5570, doi:10.1021/acs.est.7b02395, 2018b.Chiwa, M.: Ten-year determination of atmospheric phosphorus deposition at three forested sites in Japan, Atmos. Environ., 223(May 2019), 1–7, doi:10.1016/j.atmosenv.2019.117247, 2020.

Chiwa, M.: Long-term changes in atmospheric nitrogen deposition and stream water nitrate leaching from forested watersheds in western Japan, Environ. Pollut., 287(November 2020), 117634, doi:10.1016/j.envpol.2021.117634, 2021.

Chiwa, M., Enoki, T., Higashi, N., Kumagai, T. and Otsuki, K.: The Increased Contribution of Atmospheric Nitrogen Deposition to Nitrogen Cycling in a Rural

618 Forested Area of Kyushu, Japan, Water, Air, Soil Pollut., 224(11), 1763,
619 doi:10.1007/s11270-013-1763-2, 2013.
620 Chiwa, M., Onikura, N., Ide, J. and Kume, A.: Impact of N-Saturated Upland Forests
621 on Downstream N Pollution in the Tatara River Basin, Japan, Ecosystems, 15(2),
622 230–241, doi:10.1007/s10021-011-9505-z, 2012.
623 Chiwa, M.: Characteristics of atmospheric nitrogen and sulfur containing compounds
624 in an inland suburban-forested site in northern Kyushu, western Japan, Atmos. Res.,
625 96(4), 531–543, doi:10.1016/j.atmosres.2010.01.001, 2010.
626 Ding, W., Tsunogai, U., Nakagawa, F., Sambuichi, T., Sase, H., Morohashi, M., and
627 Yotsuyanagi, H.: Tracing the source of nitrate in a forested stream showing elevated
628 concentrations during storm events, Biogeosciences, 19, 3247–3261,
629 https://doi.org/10.5194/bg-19-3247-2022, 2022.
630 Endo, T., Yagoh, H., Sato, K., Matsuda, K., Hayashi, K., Noguchi, I. and Sawada, K.:
631 Regional characteristics of dry deposition of sulfur and nitrogen compounds at
632 EANET sites in Japan from 2003 to 2008, Atmos. Environ., 45(6), 1259–1267,
633 doi:10.1016/j.atmosenv.2010.12.003, 2011.
634 Farrick, K. K. and Branfireun, B. A.: Flowpaths, source water contributions and water
635 residence times in a Mexican tropical dry forest catchment, J. Hydrol., 529, 854–865,
636 doi:10.1016/j.jhydrol.2015.08.059, 2015.Kabeya, N., Shimizu, A., Nobuhiro, T. and
637 Tamai, K.: Preliminary study of flow regimes and stream water residence times in
638 multi-scale forested watersheds of central Cambodia, Paddy Water Environ., 6(1), 25–

35, doi:10.1007/s10333-008-0104-3, 2008.

Fukushima, K., Tateno, R. and Tokuchi, N.: Soil nitrogen dynamics during stand development after clear-cutting of Japanese cedar (Cryptomeria japonica) plantations, J. For. Res., 16(5), 394–404, doi:10.1007/s10310-011-0286-1, 2011.

Galloway, J. N., Aber, J. D., Erisman, J. W., Seitzinger, S. P., Howarth, R. W., Cowling, E. B. and Cosby, B. J.: The nitrogen cascade, Bioscience, 53(4), 341–356, doi:10.1641/0006-3568(2003)053[0341:TNC]2.0.CO;2, 2003.

Hattori, S., Nuñez Palma, Y., Itoh, Y., Kawasaki, M., Fujihara, Y., Takase, K. and Yoshida, N.: Isotopic evidence for seasonality of microbial internal nitrogen cycles in a temperate forested catchment with heavy snowfall, Sci. Total Environ., 690, 290–299, doi:10.1016/j.scitotenv.2019.06.507, 2019.

Hirota, A., Tsunogai, U., Komatsu, D. D. and Nakagawa, F.: Simultaneous determination of $\delta^{15}N$ and $\delta^{18}O$ of N_2O and $\delta^{13}C$ of CH_4 in nanomolar quantities from a single water sample, Rapid Commun. Mass Spectrom., 24, 1085–1092, doi:10.1002/rcm.4483, 2010.

Huang, S., Wang, F., Elliott, E. M., Zhu, F., Zhu, W., Koba, K., Yu, Z., Hobbie, E. A., Michalski, G., Kang, R., Wang, A., Zhu, J., Fu, S. and Fang, Y.: Multiyear Measurements on $\Delta^{17}O$ of Stream Nitrate Indicate High Nitrate Production in a Temperate Forest, Environ. Sci. Technol., 54(7), 4231–4239, doi:10.1021/acs.est.9b07839, 2020.

Inoue, T., Nakagawa, F., Shibata, H. and Tsunogai, U.: Vertical Changes in the Flux

660 of Atmospheric Nitrate From a Forest Canopy to the Surface Soil Based on $\Delta^{17}O$
661 Values, J. Geophys. Res. Biogeosciences, 126(4), 1–18, doi:10.1029/2020JG005876,
662 2021.
663 Inamdar, S. P. and Mitchell, M. J.: Hydrologic and topographic controls on storm-
664 event exports of dissolved organic carbon (BOC) and nitrate across catchment scales,
665 Water Resour. Res., 42(3), 1–16, doi:10.1029/2005WR004212, 2006.
666 Kaiser, J., Hastings, M. G., Houlton, B. Z., Röckmann, T. and Sigman, D. M.: Triple
667 oxygen isotope analysis of nitrate using the denitrifier method and thermal
668 decomposition of N_2O, Anal. Chem., 79(2), 599–607, doi:10.1021/ac061022s, 2007.
669 Komatsu, D. D., Ishimura, T., Nakagawa, F. and Tsunogai, U.: Determination of the
670 $^{15}N/^{14}N$, $^{17}O/^{16}O$, and $^{18}O/^{16}O$ ratios of nitrous oxide by using continuous-flow
671 isotope-ratio mass spectrometry Daisuke, Rapid Commun. Mass Spectrom., 22, 1587–
672 1596, doi:10.1002/rcm.3493, 2008a.
673 Komatsu, H., Maita, E. and Otsuki, K.: A model to estimate annual forest
674 evapotranspiration in Japan from mean annual temperature, , 330–340,
675 doi:10.1016/j.jhydrol.2007.10.006, 2008b.
676 Konno, U., Tsunogai, U., Komatsu, D. D., Daita, S., Nakagawa, F., Tsuda, A.,
677 Matsui, T., Eum, Y. J. and Suzuki, K.: Determination of total N_2 fixation rates in the
678 ocean taking into account both the particulate and filtrate fractions, Biogeosciences,
679 7(8), 2369–2377, doi:10.5194/bg-7-2369-2010, 2010.
680 Matsuda, K.: Estimation of dry deposition for sulfur and nitrogen compounds in the

681 atmosphere : Updated parameterization of deposition velocity, J. Japan Soc. Atmos.
682 Environ., 43(6), 332–339, doi:10.11298/taiki1995.43.332, 2008.
683 McIlvin, M. R. and Altabet, M. A.: Chemical conversion of nitrate and nitrite to
684 nitrous oxide for nitrogen and oxygen isotopic analysis in freshwater and seawater,
685 Anal. Chem., 77(17), 5589–5595, doi:10.1021/ac050528s, 2005.
686 Michalski, G., Scott, Z., Kabiling, M. and Thiemens, M. H.: First measurements and
687 modeling of $\Delta^{17}O$ in atmospheric nitrate, Geophys. Res. Lett., 30(16), 3–6,
688 doi:10.1029/2003GL017015, 2003.
689 Michalski, G., Meixner, T., Fenn, M., Hernandez, L., Sirulnik, A., Allen, E. and
690 Thiemens, M.: Tracing Atmospheric Nitrate Deposition in a Complex Semiarid
691 Ecosystem Using $\Delta^{17}O$, Environ. Sci. Technol., 38(7), 2175–2181,
692 doi:10.1021/es034980+, 2004.
693 Mitchell, M. J., Iwatsubo, G., Ohrui, K. and Nakagawa, Y.: Nitrogen saturation in
694 Japanese forests: An evaluation, For. Ecol. Manage., 97(1), 39–51,
695 doi:10.1016/S0378-1127(97)00047-9, 1997.
696 Morin, S., Sander, R. and Savarino, J.: Simulation of the diurnal variations of the
697 oxygen isotope anomaly ($\Delta^{17}O$) of reactive atmospheric species, Atmos. Chem. Phys.,
698 11(8), 3653–3671, doi:10.5194/acp-11-3653-2011, 2011.
699 Nakagawa, F., Suzuki, A., Daita, S., Ohyama, T., Komatsu, D. D. and Tsunogai, U.:
700 Tracing atmospheric nitrate in groundwater using triple oxygen isotopes: Evaluation
701 based on bottled drinking water, Biogeosciences, 10(6), 3547–3558, doi:10.5194/bg-

10-3547-2013, 2013.

Nakagawa, F., Tsunogai, U., Obata, Y., Ando, K., Yamashita, N., Saito, T., Uchiyama, S., Morohashi, M. and Sase, H.: Export flux of unprocessed atmospheric nitrate from temperate forested catchments: A possible new index for nitrogen saturation, Biogeosciences, 15(22), 7025–7042, doi:10.5194/bg-15-7025-2018, 2018.

Nelson, D. M., Tsunogai, U., Ding, D., Ohyama, T., Komatsu, D. D., Nakagawa, F., Noguchi, I. and Yamaguchi, T.: Triple oxygen isotopes indicate urbanization affects sources of nitrate in wet and dry atmospheric deposition, Atmos. Chem. Phys., 18(9), 6381–6392, doi:10.5194/acp-18-6381-2018, 2018.

Ohrui, K. and Mitchell, M. J.: Nitrogen Saturation in Japanese Forested Watersheds Author (s): Kiyokazu Ohrui and Myron J . Mitchell Published by : Wiley Stable URL : http://www.jstor.org/stable/2269507 Accessed : 05-07-2016 04 : 51 UTC Your use of the JSTOR archive indicates your ac, , 7(2), 391–401, 1997.

Paerl, H. W. and Huisman, J.: Climate change: A catalyst for global expansion of harmful cyanobacterial blooms, Environ. Microbiol. Rep., 1(1), 27–37, doi:10.1111/j.1758-2229.2008.00004.x, 2009.

Peterjohn, W. T., Adams, M. B. and Gilliam, F. S.: Symptoms of nitrogen saturation in two central Appalachian hardwood forest ecosystems, Biogeochemistry, 35(3), 507–522, doi:10.1007/BF02183038, 1996.

Riha, K. M., Michalski, G., Gallo, E. L., Lohse, K. A., Brooks, P. D. and Meixner, T.: High Atmospheric Nitrate Inputs and Nitrogen Turnover in Semi-arid Urban

723 Catchments, Ecosystems, 17(8), 1309–1325, doi:10.1007/s10021-014-9797-x, 2014.
724 Rodgers, P., Soulsby, C., Waldron, S. and Tetzlaff, D.: Using stable isotope tracers to
725 identify hydrological flow paths, residence times and landscape controls in a
726 mesoscale catchment, Hydrol. Earth Syst. Sci. Discuss., 9, 139–155, 2005.Rose, L.
727 A., Elliott, E. M. and Adams, M. B.: Triple Nitrate Isotopes Indicate Differing Nitrate
728 Source Contributions to Streams Across a Nitrogen Saturation Gradient, Ecosystems,
729 18(7), 1209–1223, doi:10.1007/s10021-015-9891-8, 2015.
730 Sabo, R. D., Nelson, D. M. and Eshleman, K. N.: Episodic, seasonal, and annual
731 export of atmospheric and microbial nitrate from a temperate forest, Geophys. Res.
732 Lett., 43(2), 683–691, doi:10.1002/2015GL066758, 2016.
733 Sappa, G., Ferranti, F. and Pecchia, G. M.: Validation Of Salt Dilution Method For
734 Discharge Measurements In The Upper Valley Of Aniene River (Central Italy), Recent
735 Adv. Environ. Ecosyst. Dev., (October 2015), 42–48, 2015.
736 Soulsby, C., Tetzlaff, D., Rodgers, P., Dunn, S. and Waldron, S.: Runoff processes,
737 stream water residence times and controlling landscape characteristics in a mesoscale
738 catchment: An initial evaluation, J. Hydrol., 325(1–4), 197–221,
739 doi:10.1016/j.jhydrol.2005.10.024, 2006.
740 Stoddard, J. L.: Long-Term Changes in Watershed Retention of Nitrogen, , 223–284,
741 doi:10.1021/ba-1994-0237.ch008, 1994.
742 Tetzlaff, D., Malcolm, I. A. and Soulsby, C.: Influence of forestry, environmental
743 change and climatic variability on the hydrology, hydrochemistry and residence times

744 of upland catchments, J. Hydrol., 346(3–4), 93–111,
745 doi:10.1016/j.jhydrol.2007.08.016, 2007.
746 Tsunogai, U., Komatsu, D. D., Daita, S., Kazemi, G. A., Nakagawa, F., Noguchi, I.
747 and Zhang, J.: Tracing the fate of atmospheric nitrate deposited onto a forest
748 ecosystem in Eastern Asia using $\Delta^{17}O$, Atmos. Chem. Phys., 10(4), 1809–1820,
749 doi:10.5194/acp-10-1809-2010, 2010.
750 Tsunogai, U., Daita, S., Komatsu, D. D., Nakagawa, F. and Tanaka, A.: Quantifying
751 nitrate dynamics in an oligotrophic lake using $\Delta^{17}O$, Biogeosciences, 8(3), 687–702,
752 doi:10.5194/bg-8-687-2011, 2011.
753 Tsunogai, U., Komatsu, D. D., Ohyama, T., Suzuki, A., Nakagawa, F., Noguchi, I.,
754 Takagi, K. and Nomura, M.: Quantifying the effects of clear-cutting and strip-cutting
755 on nitrate dynamics in a forested watershed using triple oxygen isotopes as tracers, ,
756 (1), 5411–5424, doi:10.5194/bg-11-5411-2014, 2014.
757 Tsunogai, U., Miyauchi, T., Ohyama, T., Komatsu, D. D., Nakagawa, F., Obata, Y.,
758 Sato, K. and Ohizumi, T.: Accurate and precise quantification of atmospheric nitrate
759 in streams draining land of various uses by using triple oxygen isotopes as tracers,
760 Biogeosciences, 13(11), 3441–3459, doi:10.5194/bg-13-3441-2016, 2016.
761 Tsunogai, U., Miyauchi, T., Ohyama, T., Komatsu, D. D., Ito, M. and Nakagawa, F.:
762 Quantifying nitrate dynamics in a mesotrophic lake using triple oxygen isotopes as
763 tracers, Limnol. Oceanogr., 63, S458–S476, doi:10.1002/lno.10775, 2018.
764 Vitousek, P. M. and Howarth, R. W.: Nitrogen limitation on land and in the sea: How

765 can it occur?, Biogeochemistry, 13(2), 87–115, doi:10.1007/BF00002772, 1991.
766 Watanabe, M., Miura, S., Hasegawa, S., Koshikawa, M. K., Takamatsu, T., Kohzu,
767 A., Imai, A. and Hayashi, S.: Coniferous coverage as well as catchment steepness
768 influences local stream nitrate concentrations within a nitrogen-saturated forest in
769 central Japan, Sci. Total Environ., 636, 539–546, doi:10.1016/j.scitotenv.2018.04.307,
770 2018.
771 Yamazaki, A., Watanabe, T. and Tsunogai, U.: Nitrogen isotopes of organic nitrogen
772 in reef coral skeletons as a proxy of tropical nutrient dynamics, Geophys. Res. Lett.,
773 38(19), 1–5, doi:10.1029/2011GL049053, 2011.
774 Yang, R. and Chiwa, M.: Low nitrogen retention in a Japanese cedar plantation in a
775 suburban area, western Japan, Sci. Rep., 11(1), 1–7, doi:10.1038/s41598-021-84753-
776 1, 2021.
777
778
779
780
781
782
783
784
785

786 **Table 1.** Plant information for each forested catchment (Chiwa, 2021).

Overstory vegetation (%)	FK1	FK2	MY
Artificial Japanese cedar/cypress plantation	74	40	16
Other artificial coniferous plantations	<1	<1	7
Natural trees	10	54	75
Others	16	5	2

787

788

789

790 **Table 2.** Average concentrations of stream nitrate ($[NO_3^-]_{avg}$), the average
791 concentrations of unprocessed $NO_3^-{}_{atm}$ in streams ($[NO_3^-{}_{atm}]_{avg}$), the annual export flux
792 of NO_3^- per unit area of catchments (M_{total}), the annual export flux of $NO_3^-{}_{atm}$ per unit
793 area of catchments (M_{atm}), the deposition flux of $NO_3^-{}_{atm}$ per unit area of catchment
794 (D_{atm}), and the M_{atm}/D_{atm} ratios in the study catchments.

	FK1	FK2	MY
$[NO_3^-]_{avg}$ (μM)	109.5	90.9	7.3
$[NO_3^-{}_{atm}]_{avg}$ (μM)	10.80 ± 1.30	5.06 ± 0.67	0.16 ± 0.03
M_{total} (mmol m^{-2} yr^{-1})	98.8 ± 17.8	82.0 ± 14.8	23.7 ± 1.2
M_{atm} (mmol m^{-2} yr^{-1})	9.7 ± 2.1	4.6 ± 1.0	0.5 ± 0.1
D_{atm} (mmol m^{-2} yr^{-1})	69.3 ± 13.9	69.3 ± 13.9	40.1 ±8.0
M_{atm}/D_{atm} (%)	14.1 ± 4.1	6.6 ± 2.0	1.3 ± 0.4

795

Table 3. The annual amount of precipitation (P), the average concentration of stream nitrate ($[NO_3^-]_{avg}$), the nitrogen saturation stage, the average concentration of unprocessed $NO_3^-{}_{atm}$ in streams ($[NO_3^-{}_{atm}]_{avg}$), the annual export flux of NO_3^- per unit area of catchment (M_{total}), the annual export flux of $NO_3^-{}_{atm}$ per unit area of catchment (M_{atm}), the deposition flux of $NO_3^-{}_{atm}$ per unit area of catchment (D_{atm}), and the M_{atm}/D_{atm} ratio in the FK1, FK2, and MY, along with those in the catchments studied in past studies using $\Delta^{17}O$ of nitrate as a tracer.

	P	$[NO_3^-]_{avg}$	N stage*	$[NO_3^-{}_{atm}]_{avg}$	M_{atm}	M_{total}	D_{atm}	M_{atm}/D_{atm}
	mm	μM		μM	mmol m^{-2} yr^{-1}			%
FK1[a]	1777	109.5	-	10.8	9.7	98.8	69.3	14.1
FK2[a]	1777	90.9	-	5.06	4.6	82.0	69.3	6.6
MY[a]	3981	7.3	-	0.2	0.5	23.7	40.1	1.3
KJ[b]	2500	58.4	-	3.3	4.3	76.4	45.6	9.4
IJ1[b]	3300	24.4	2	1.4	2.9	50.1	44.5	6.5
IJ2[b]	3300	17.1	-	0.6	1.2	35.1	44.5	2.6
Fernow1[c]	1450	17.9	1	1.6	0.8	9.3	23.4	3.6
Fernow2[c]	1450	34.3	2	3.4	1.5	14.8	23.4	6.3
Fernow3[c]	1450	60.0	3	4.2	2.4	34.5	23.4	10.3
Uryu[d]	1170	0.7	-	0.1	0.1	1.0	18.6	0.7
Qingyuan[e]	709	150.0	2	8.9	2.9	49.3	50.0	5.8

a: This study
b: Nakagawa et al., 2018; Nakahara et al., 2010
c: Rose et al., 2015
d: Tsunogai et al., 2014
e: Huang et al., 2020
*: N saturation stage estimated in past studies
-: No data

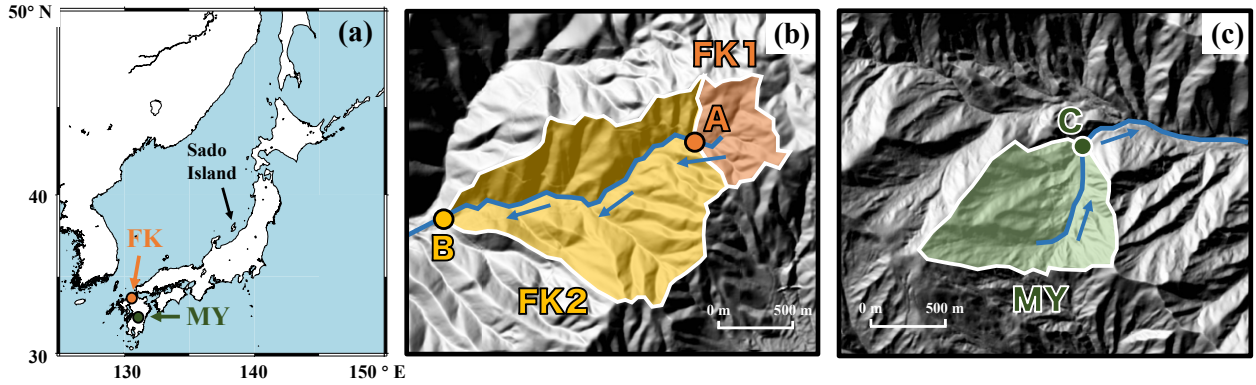

Figure 1. A map showing the locations of the study catchments (FK and MY) in Japan (a), and the maps of FK1, FK2 (b) and MY catchments (c), shown by orange, yellow, and green areas, respectively, together with the sampling station A, B, and C, respectively, shown by orange, yellow, and green circles, respectively. The blue arrows indicate the flow direction of stream water.

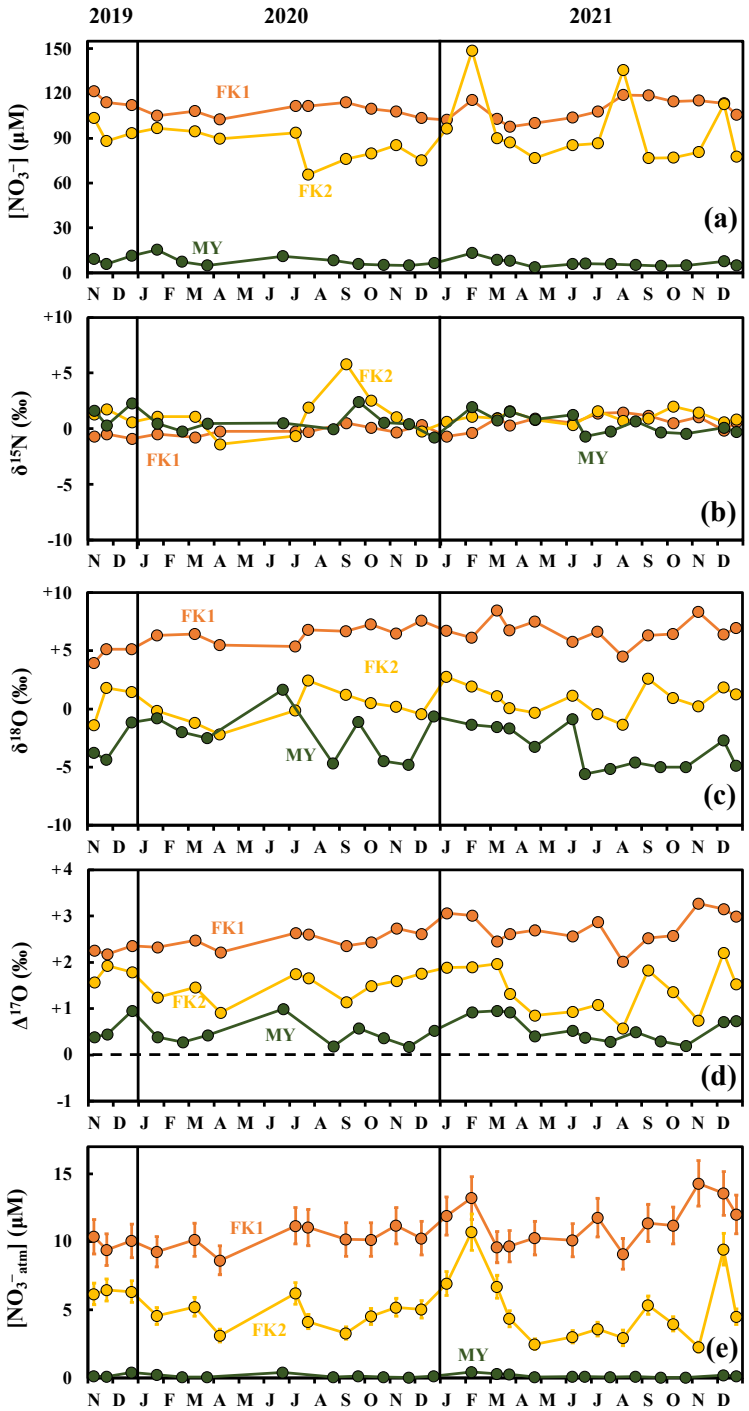

Figure 2. Temporal variations in concentrations of stream nitrate (FK1: orange circles; FK2: yellow circles; MY: green circles) (a), together with those in $\delta^{15}N$ (b), $\delta^{18}O$ (c), and $\Delta^{17}O$ (d) of nitrate, and the concentration of unprocessed $NO_3^-_{atm}$ ($[NO_3^-_{atm}]$) (e) in the stream water of the FK1, FK2, and MY forested catchments. Error bars smaller than the sizes of the symbols are not presented.

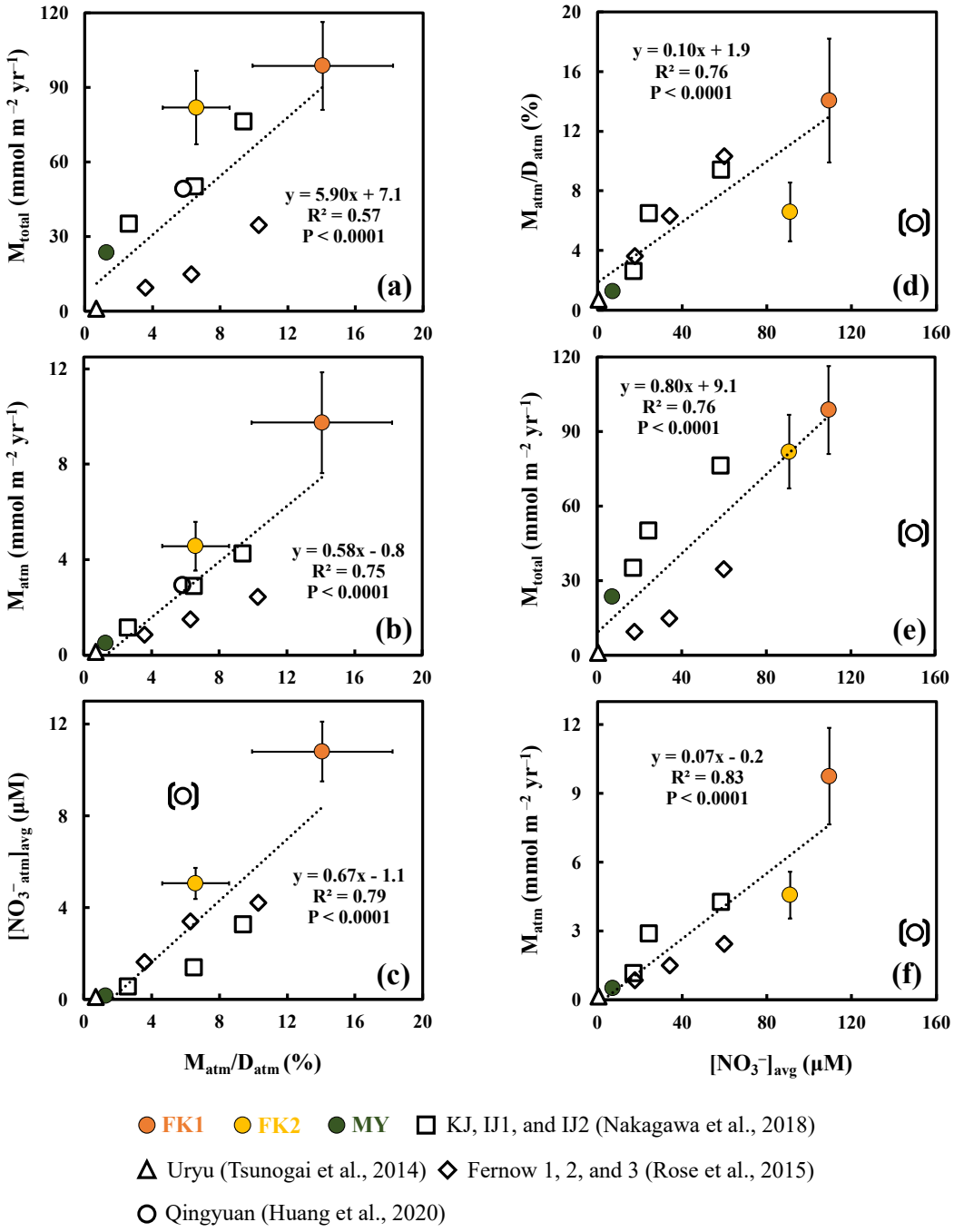

Figure 3. Annual export flux of nitrate per unit area (M_{total}) plotted as a function of the M_{atm}/D_{atm} ratio in each forested catchment (a); the annual export flux of unprocessed atmospheric nitrate per unit area (M_{atm}) plotted as a function of the M_{atm}/D_{atm} ratio (b); the average concentration of $NO_3^-{}_{atm}$ ($[NO_3^-{}_{atm}]_{avg}$) plotted as a function of the M_{atm}/D_{atm} ratio (c); the M_{atm}/D_{atm} ratio plotted as a function of the average concentration

825 of nitrate ($[NO_3^-]_{avg}$) (d); the M_{total} plotted as a function of $[NO_3^-]_{avg}$ (e); the M_{atm}
826 plotted as a function of $[NO_3^-]_{avg}$ (f) (FK1: orange circles; FK2: yellow circles; MY:
827 green circles). Those determined for the forested catchments in past studies are plotted
828 as well (Qingyuan: white circle (Huang et al., 2020); KJ, IJ1, and IJ2: white squares
829 (Nakagawa et al., 2018); Fernow 1, 2, and 3: white diamonds (Lucy et al., 2015); Uryu:
830 white triangle (Tsunogai., 2014)). The data obtained in the Qingyuan forested
831 catchment are shown in parentheses and excluded from the calculation to estimate
832 correlation coefficients (see text for the reason).

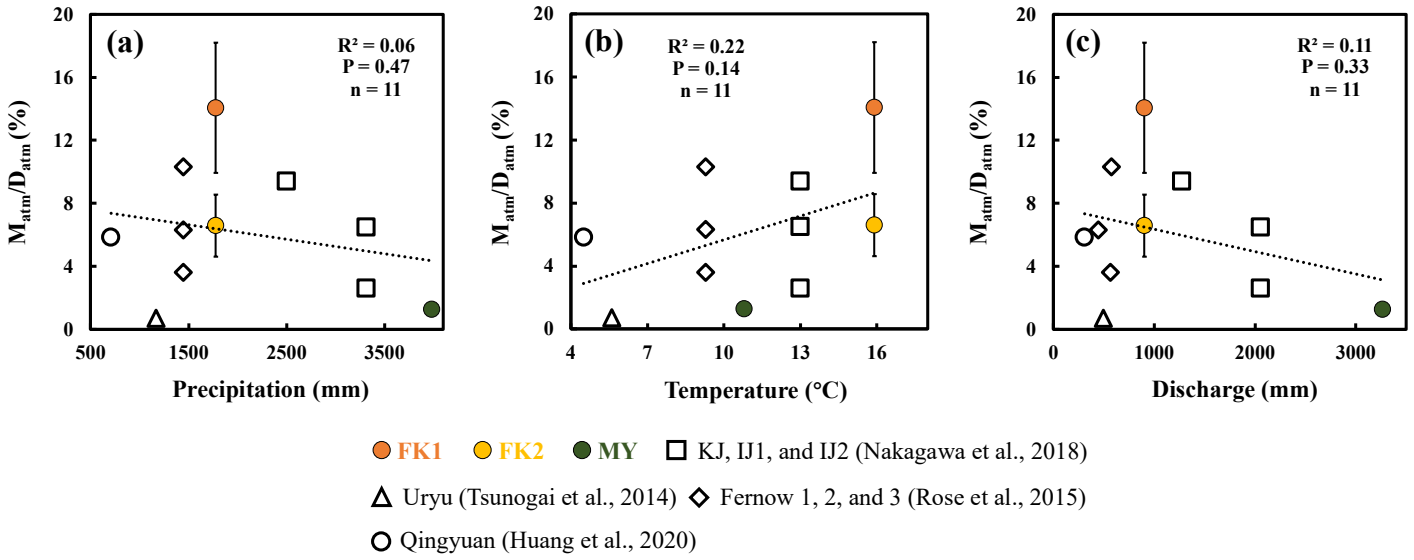

833 **Figure 4.** the M_{atm}/D_{atm} ratio plotted as a function of the amount of precipitation (a),
834 the M_{atm}/D_{atm} ratio plotted as a function of the temperature (b), and the M_{atm}/D_{atm} ratio
835 plotted as a function of flux of stream water (c) (FK1: orange circles; FK2: yellow
836 circles; MY: green circles). Those determined for the forested catchments in past studies
837 are plotted as well.
838

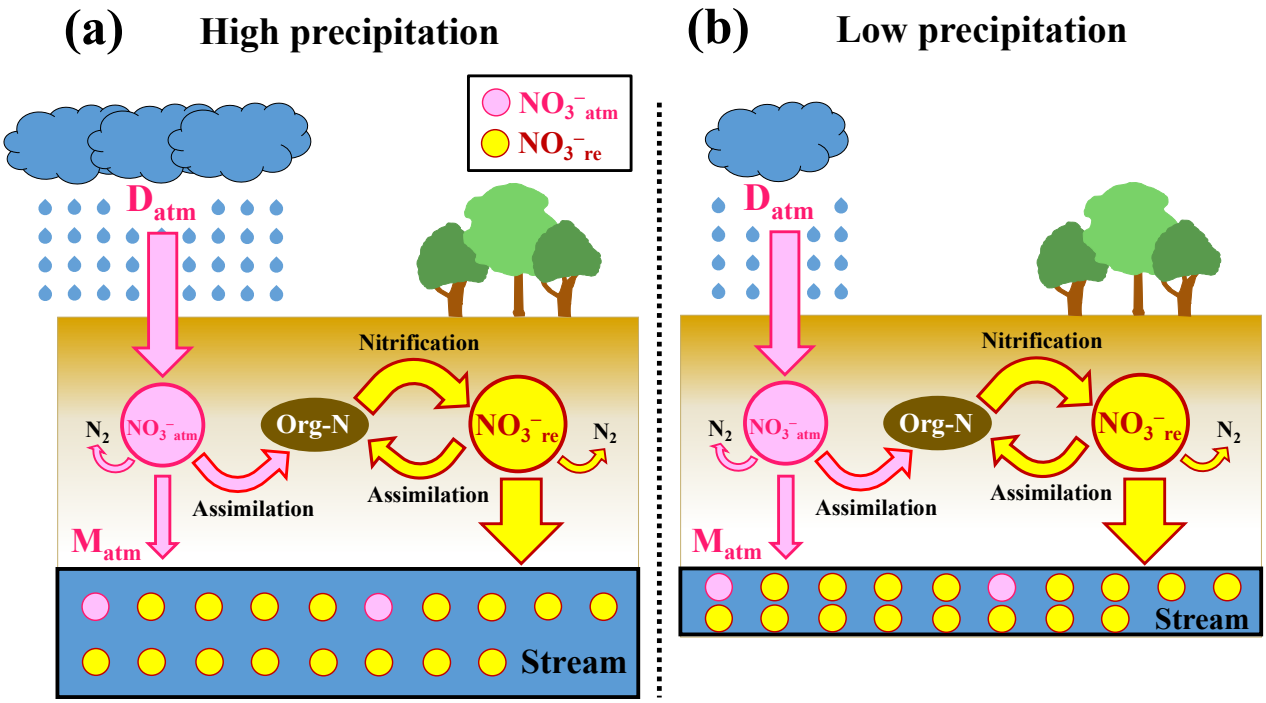

839 **Figure 5.** Schematic diagram showing the biogeochemical processing of nitrate in
840 forested catchments under high precipitation (a) and low precipitation (b), where
841 $NO_3^-_{atm}$ (unprocessed atmospheric nitrate) is represented by pink circles, $NO_3^-_{re}$ by
842 yellow circles, the flows of $NO_3^-_{atm}$ by pink arrows, and those of $NO_3^-_{re}$ (remineralized
843 nitrate) by yellow arrows (modified after Nakagawa., 2018). Although the deposition
844 rates of $NO_3^-_{atm}$ (D_{atm}) and the biogeochemical reaction rates between (a) and (b) are
845 the same, we can expect high [NO_3^-] in (b). On the other hand, the M_{atm}/D_{atm} ratio
846 between (a) and (b) are the same.